Electronic Supplementary Material (ESI) for Chemical Science.

Supporting Information for the manuscript:

Switchable slow relaxation of magnetization in the native low temperature phase of a cooperative spin-crossover compound

A. Urtizberea and O. Roubeau

Table of contents

Synthesis

1-methyl-tetrazole (mtz). The ligand mtz was synthesized as described previously.[1]

$[Fe(mtz)_6](CF_6SO_3)_2$ (2). Two slightly different methods were used.

Method 1. 50 mg of $[Fe(H_2O)_6](CF_3SO_3)_2$ (obtained by reacting Fe powder in 2M aqueous solution of trifluorosulfonic acid, 0.11 mmol), 2 mg ascorbic acid and 70 of mtz (0.83 mmol) are dissolved in 10 mL absolute EtOH and the solution boiled for 10 min. The solution is let cool down and evaporate under ambient conditions. Large colorless crystals form when the solution has almost completely evaporated. The remaining solution and crystals are taken over with little diethyl ether, recovered by filtration and washed with a 3:1 EtOH:diethylether mixture. The yield is 81 mg (86 % based on Fe).

Method 2. 238 mg of commercial $Fe(CF_3SO_3)_2$ (Aldrich, 85 %, 0.57 mmol), 5 mg ascorbic acid and 310 mg of mtz (3.69 mmol) are dissolved in a mixture of absolute ethanol (15 mL) and triethylorthoformate (10 mL). The reaction mixture is stirred at room temperature for 15 min, and let evaporate under ambient conditions. Colorless crystals form when the solution has almost completely evaporated. The formed crystals and polycrystalline powder are recovered by filtration and washed with a 3:1 EtOH:diethylether mixture. The yield is 345 mg (70 % based on Fe).

As reported,[2] the solids can be recrystallized from nitromethane (we used 11 mg in 3 mL). We however found no difference in the products obtained by the two methods and after re-crystallization, based on single-crystal and powder diffraction, IR spectroscopy and elemental analysis. Anal. Calc. (Found) for $FeC_{14}H_{24}N_{24}O_6F_6S_2$: C, 19.59 (19.7); H, 2.82 (2.9); N, 39.16 (38.9).

$[Fe(mtz)_6](BF_4)_2$ (3).

237 mg of commercial $Fe(BF_4)_2{\cdot}6H_2O$ (Aldrich, 97 %, 0.7 mmol), 5 mg ascorbic acid and 390 mg of mtz (4.6 mmol) are dissolved in a mixture of absolute ethanol (15 mL) and triethylorthoformate (10 mL). The reaction mixture is stirred at room temperature for 15 min, resulting in the formation of small amounts of a white suspension. After removing the white solid by filtration (< 10 mg), the filtrate is let evaporate slowly under ambient conditions and a fine microcrystalline white solid deposits. The solid formed after 48 hours is recovered by filtration and washed with a 1:1 EtOH:diethylether mixture. The yield is 195 mg (32 % based on Fe). A second crop can be recovered from the filtrate but was not isolated. Phase purity was checked by powder x-ray diffraction and IR spectroscopy.

Magnetic measurements.

Magnetic measurements were performed using Quantum Design SQUID magnetometers (MPMS-XL, MPMS-5S) and PPMS platform equipped with the ACMS susceptibility option, through the Physical Measurements unit of the Servicio de Apoyo a la Investigación-SAI, Universidad de Zaragoza.

MPMS-XL was used for *dc* measurements in the temperature range between 2 and 210 K and under magnetic fields up to 50 kOe as well as for an initial evaluation of the *ac* susceptibility *vs.* field and frequency at 2 K. Further *ac* susceptibility at variable temperature, field and frequency were then obtained with the PPMS set-up as it allows acquiring data up to higher frequencies (10 kHz).

Polycrystalline powder was mixed with apiezon N grease to prevent sample grains from moving under the action of magnetic field, for *dc* measurements up to 50 kOe at low temperatures.

Irradiation studies were done with the MPMS-5S and the commercial FiberOptic Sample Holder (FOSH) in combination with a Xe arc lamp and short-pass and long-pass interference filters, specifically LPF650-SPF900 and LPF500-SPF650 respectively for red (650-900 nm) and green (500-650) broad-band irradiations. The sample was then in the form of a small piece of a very thin 0.7 mm diameter pellet, to minimize the effect of the attenuation of the propagation of light through the sample.

All data were corrected for the sample holders and grease contributions, determined empirically as well as for the intrinsic diamagnetism of the sample, estimated using Pascal constants.

Single Crystal X-ray Diffraction.

Data were collected on Beamline 11.3.1 at the Advanced Light Source, on a Bruker D8 diffractometer using silicon 111 monochromated synchrotron radiation (λ = 0.7749 Å). A colorless block crystal of dimensions 0.10 x 0.07 x 0.04 mm^3 was mounted on a MiTegen kapton loop at room temperature and placed in the N_2 stream at 200 K. Measurements were performed at 200 K and 85 K after slowly cooling from 200 K at *ca.* 60 K/hour. At 85 K, the crystal was light purple. Data reduction and absorption corrections were performed with SAINT and SADABS, respectively.[3] The structures were solved by intrinsic phasing with SHELXT[4] and refined by full-matrix least-squares on F^2 with SHELXL-2014.[5] All details can be found in CCDC 1493439-1493440 (**200 K-85 K**) that contain the supplementary crystallographic data for this paper. These data can be obtained free of charge from The Cambridge Crystallographic Data Center via https://summary.ccdc.cam.ac.uk/structure-summary-form. Crystallographic and refinement parameters are summarized in Table S1. Selected bond lengths and angles and intermolecular distances are given in Tables S2 and S3.

[1] P. L. Franke, J. G. Haasnoot, A. P. Zuur, *Inorg. Chim. Acta* **1982**, 59, 5-9

[2] P. Gütlich, P. Poganiuch, *Angew. Chem. Int. Ed. Engl.* **1991**, 30, 975-977

[3] G. M. Sheldrick, 2012, *SAINT and SADABS*, Bruker AXS Inc., Madison, Wisconsin, USA

[4] G. M. Sheldrick, *Acta Crystallogr. A*, **2015**, 71, 3-8

[5] G. M. Sheldrick, *Acta Crystallogr. C*, **2015**, 71, 3-8

Table S1. Crystallographic and refinement parameters for the structures of $[Fe(mtz)_6](CF_6SO_3)_2$ (**2**) at 200 and 85 K.

Formula	$C_{14}H_{24}F_6FeN_{24}O_6S_2$	
FW (g mol^{-1})	858.54	
Wavelength (Å)	0.7749	
T (K)	200	85
Crystal system	triclinic	trigonal
Space group	P–1	R–3
a (Å)	7.5430(10)	19.724(4)
b (Å)	11.336(2)	19.724(4)
c (Å)	11.424(2)	45.031(9)
α (°)	63.483(3)	90
β (°)	89.755(4)	90
γ (°)	88.763(4)	120
V (Å^3)	873.9(2)	15172(7)
Z	1	18
ρ_{calcd} (g cm^{-3})	1.631	1.691
μ (mm^{-1})	0.820	0.850
Independent reflections (R_{int})	5098 (0.0393)	4360 (0.049)
Restraints / Parameters	272 / 317	0 / 484
Goodness-of-fit on F^2	1.048	1.082
Final R_1 / wR_2 [$I>2\sigma(I)$]	0.0509 / 0.1353	0.0403 / 0.0940
Final R_1 / wR_2 [all data]	0.0652 / 0.1457	0.0609 / 0.1087
Largest diff. peak and hole (e Å^3)	0.825 / –0.663	0.245 / –0.325

Table S2. Selected bond lengths (Å) and angles (°) describing the coordination environments of the Fe sites in the structures of $[Fe(mtz)_6](CF_3SO_3)_2$ (**2**). Shorter Fe–N bond lengths associated with the LS state of Fe1 site at 85 K are highlighted in bold.

T = 200 K		*T* = 85 K	
Fe1–N1	2.1712(18)	Fe1–N1	**1.985(3)**
Fe1–N5	2.1975(17)	Fe1–N5	**1.983(3)**
Fe1–N9	2.1852(18)	Fe2–N9	2.181(3)
N1–Fe1–N5	90.59(7)	Fe2–N13	2.183(3)
N1–Fe1–N9	91.25(7)	Fe3–N17	2.221(3)
N5–Fe1–N9	88.93(7)	Fe3–N21	2.163(3)
N1–Fe1–N5#1	89.41(7)	N1 Fe1 N1#2	90.76(11)
N1–Fe1–N9#1	88.75(7)	N5 Fe1 N5#2	90.53(11)
N5–Fe1–N9#1	91.07(7)	N1 Fe1 N5	88.49(11)
		N1 Fe1 N5#2	90.23(11)
		N9 Fe2 N9#2	89.82(11)
		N13 Fe2 N13#2	89.35(11)
		N9 Fe2 N13	92.04(11)
		N9 Fe2 N13#2	88.83(11)
		N17 Fe3 N17#2	87.42(11)
		N21 Fe3 N21#2	91.89(11)
		N17 Fe3 N21	88.95(11)
		N17 Fe3 N21#2	91.68(10)

Symmetry operations: #1, -x, -y, -x; #2, -y, x-y, z.

Table S3. Selected interatomic distances (Å) describing supramolecular interactions and packing in the structures of $[Fe(mtz)_6](CF_3SO_3)_2$ (**2**) (see Figures S1-S3).

T = 200 K		T = 85 K	
“in-layer” and “inter-layer” Fe···Fe separations			
Fe1···Fe1#1	7.543	Fe1···Fe1#	7.207
Fe1···Fe1#2	11.336	Fe1···Fe3#	7.620
Fe1···Fe1#3	11.424	Fe2···Fe3#	7.329
Fe1···Fe1#4	11.974	Fe2···Fe3#	7.925
		Fe1···Fe2	11.388
		Fe1···Fe3	11.391
		Fe2···Fe3	11.391
“in-layer” C_{tz}–H···A hydrogen bonds			
C1–H1A···O3#5	2.293	C1–H1A···O1#8	2.349
C3–H3A···F3#6	2.621	C3–H3A···O5#9	2.359
C5–H5A···O1#7	2.428	C5–H5A···O4#10	2.283
		C7–H7A···F1	2.494
		C9–H9A···F6#9	2.669
		C11–H11A···O3#9	2.349
“inter-layer” C_{Me}–H···A hydrogen bonds			
C2–H2A···O2#11	2.435	C2–H2C···O2#13	2.536
C4–H4A···O2#1	2.498	C8–H8B···O2#14	2.446
C6–H6A···O2#12	2.641	C8–H8C···F3#14	2.618
		C12–H12C···O2#14	2.438

Symmetry operations: #1, x+1, y, z; #2, x, y+1, z; #3, x, y, z+1; #4, x, y+1, z-1; #5, 1-x, 1-y, 1-z; #6, 1-x, 1-y, -z; #7, 1-x, -y, 1-z; #8, -x+y, 1-x, z; #9, 1-x+y, 1-x, z; #10, -x+y, -x, z; #11, 1+x, 1+y, z; #12, 1+x, y, 1+z; #13, 2/3+x-y, 1/3+x, 4/3-z; #14, 2/3-x, 1/3-y, 4/3-z.

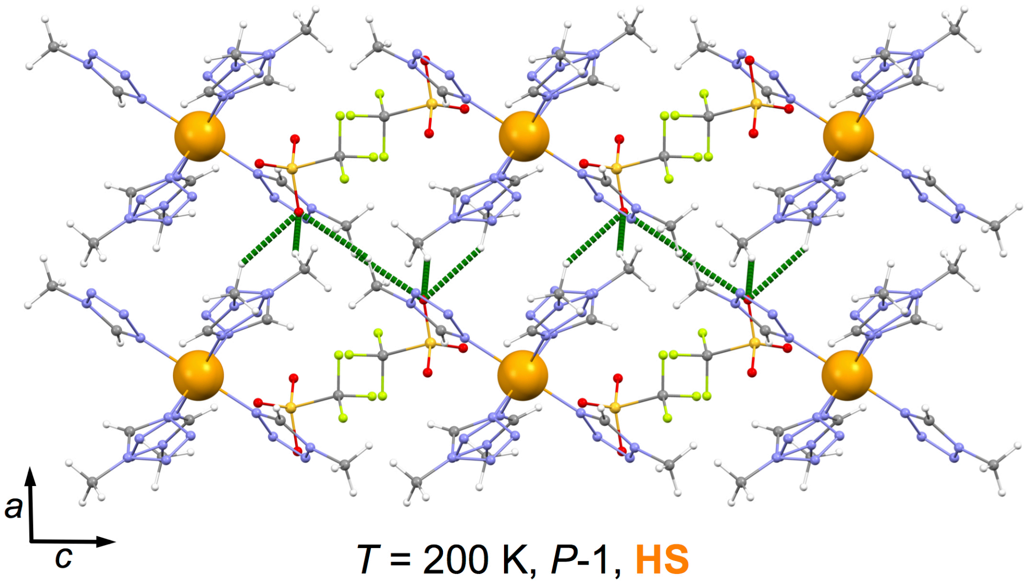

T = 200 K, *P*-1, **HS**

T = 85 K, *R*-3, 1 **LS** : 2 **HS**

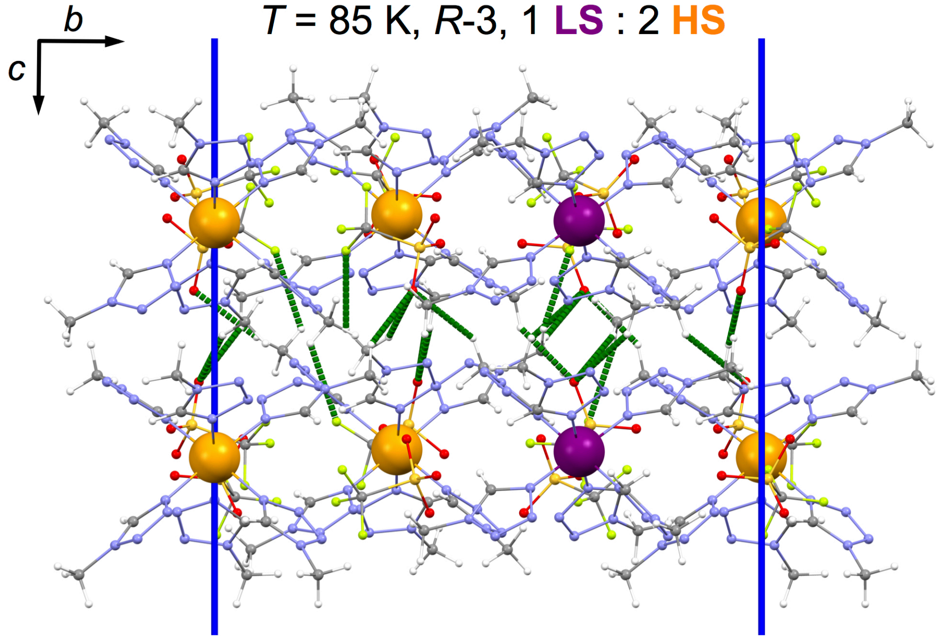

Figure S1. Views of the structure of **2** along the *b* axis at 200 K (top) and along the *a* axis at 85 K (bottom) showing the intermolecular interactions between $[Fe(mtz)_6]^{2+}$ layers through C_{Me}–H···A hydrogen bonds (green thick dashed lines). See Table S3 for details. Colour code: large orange balls Fe(II) HS; large purple ball Fe(II) LS; small light blue balls, N; small grey balls, C; small white balls, H.

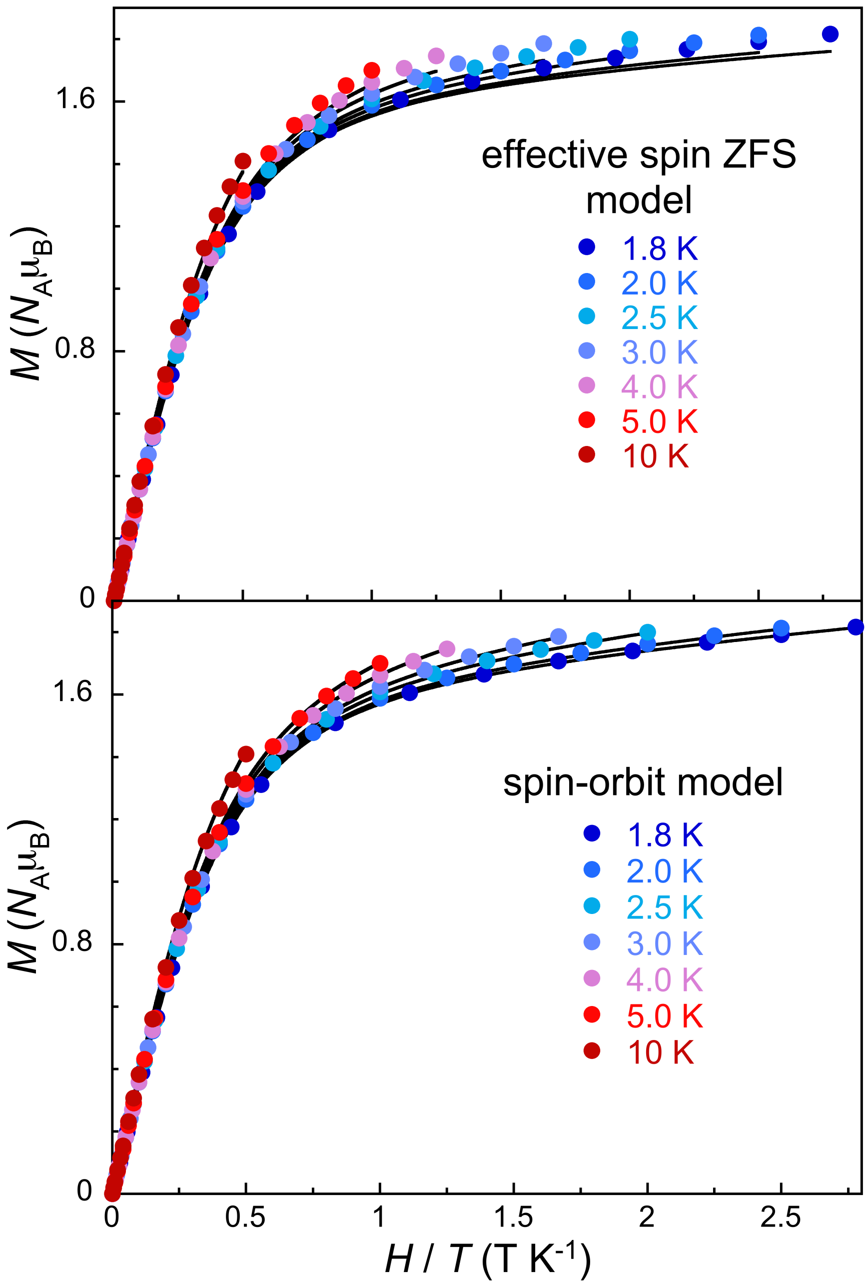

Figure S2. Magnetization isotherms *vs.* reduced field H/T at the indicated temperatures evidencing the non-superposition characteristic of significant magnetic anisotropy. Black lines are the fit of the data following (top) the effective spin ZFS model and (bottom) that including a spin-orbit term (see text).

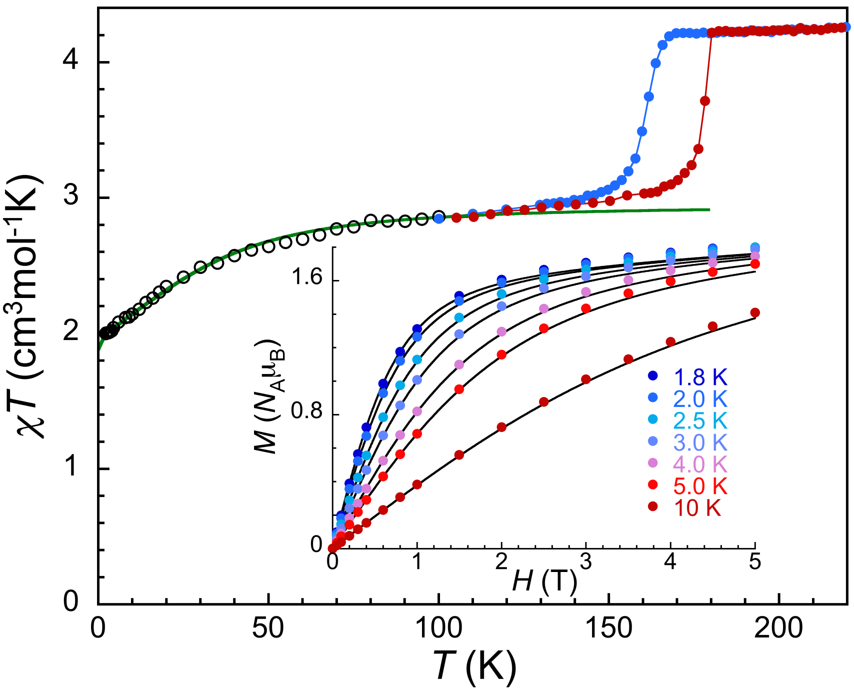

Figure S3. Temperature dependence of the χT product of **2** as derived from *dc* measurements at 0.3 K/min and 0.5 T applied *dc* field (red and blue symbols respectively in cooling and warming mode) and *ac* measurements at 15 Hz in zero-field (empty symbols). Inset: Magnetization isotherms at the indicated temperatures. Green and black lines are the fit of the data following the spin Hamilatonian (see text) through PHI software[6]

[6] N. F. Chilton, R. P. Anderson, L. D. Turner, A. Soncini, K. S. Murray, *J. Comput. Chem.* **2013**, 34, 1164-1175

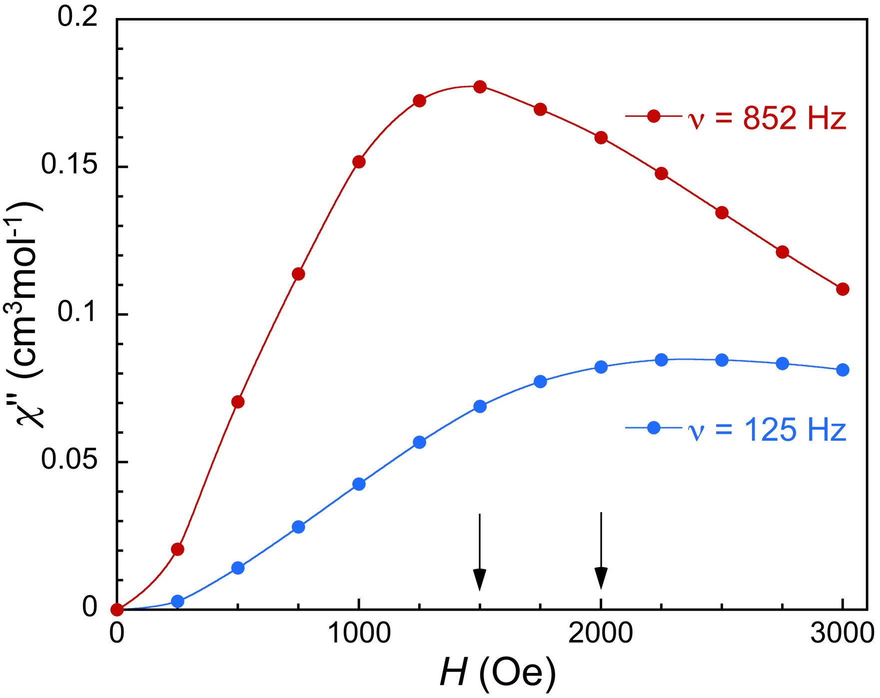

Figure S4. Evolution of the out-of-phase magnetic susceptibility χ'' of **2** at *T* = 2 K for increasing applied *dc* fields used to define optimal *dc* fields for the slow relaxation of magnetization. Arrows indicate the two fields at which further isothermal frequency dependent studies were performed.

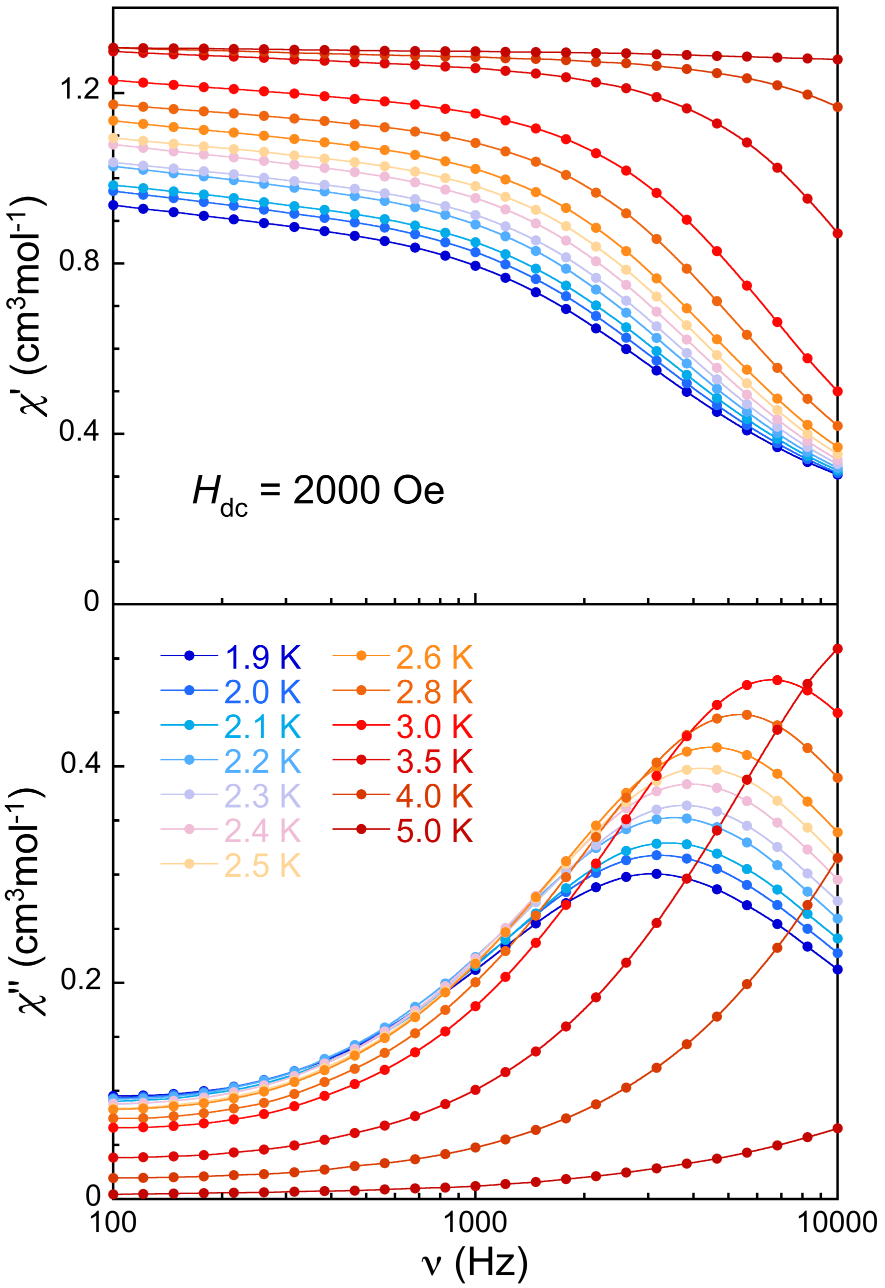

Figure S5. Frequency dependence of the in-phase (top) and out-of-phase (bottom) components of the *ac* magnetic susceptibility of **2** under a 2000 Oe applied *dc* field. The *ac* field amplitude was 4 Oe. Solid lines are guides for the eye.

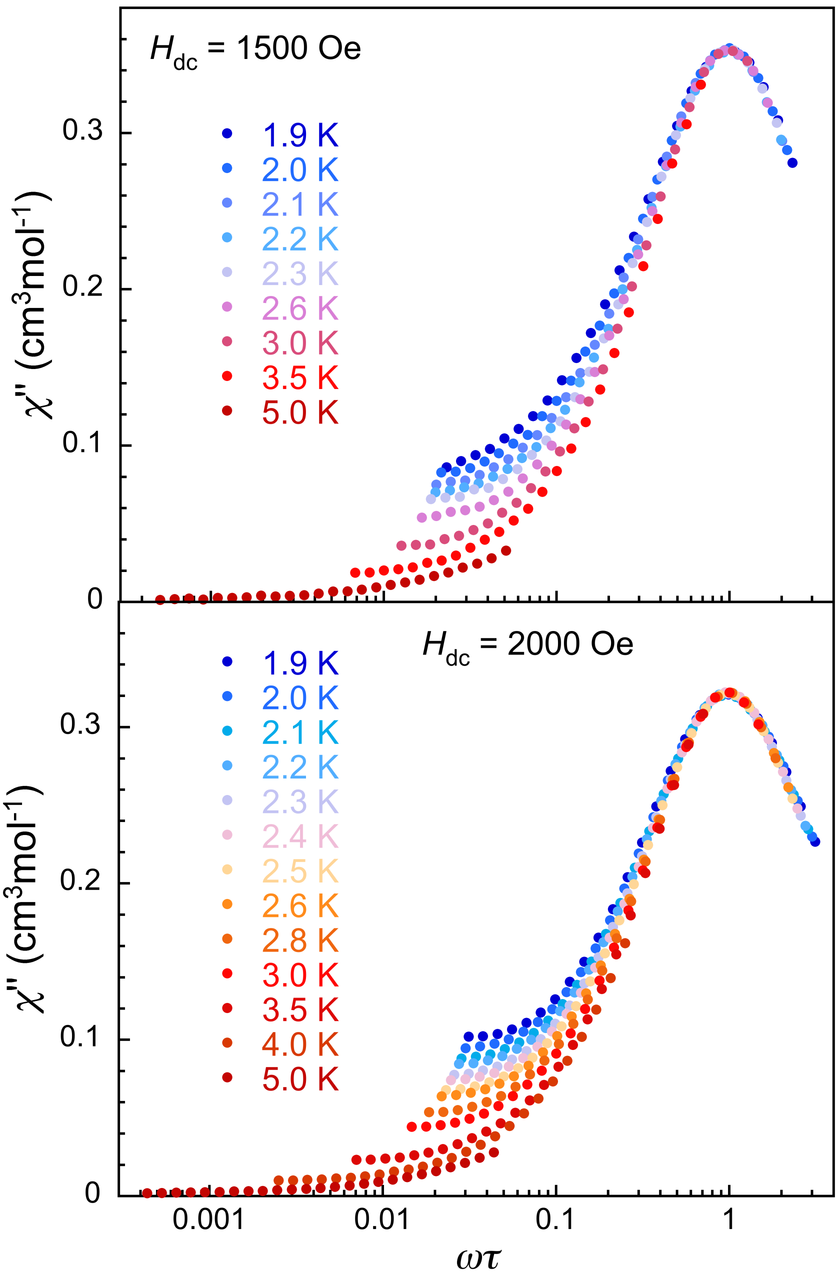

Figure S6. Frequency dependence of the scaled out-of-phase components of the *ac* magnetic susceptibility of **2** under a 1500 (top) and 2000 (bottom) Oe applied *dc* field, allowing to determine the characteristic relaxation time τ at each temperature. τ has also been obtained by performing Cole–Cole fits of the frequency dependent susceptibility data (see Fig. S7 data at 2000 Oe). The results coincide within errors with those obtained using the present scaling method.

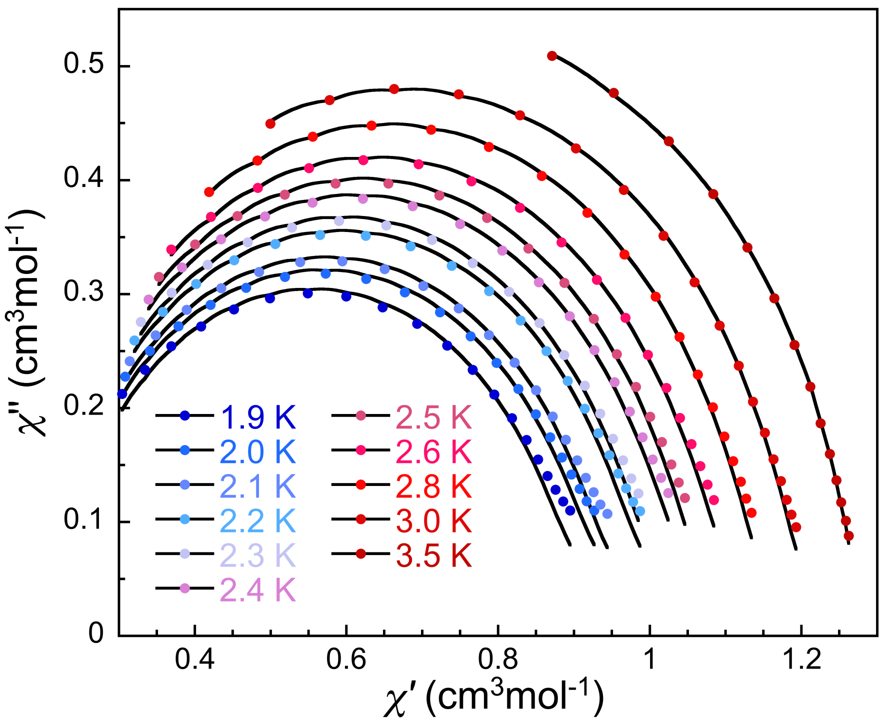

Figure S7. Cole-Cole plot of the *ac* magnetic susceptibility of **2** under a 2000 Oe applied *dc* field. Full lines are fits to the generalized Debye model allowing to determine the characteristic relaxation time τ at each temperature.

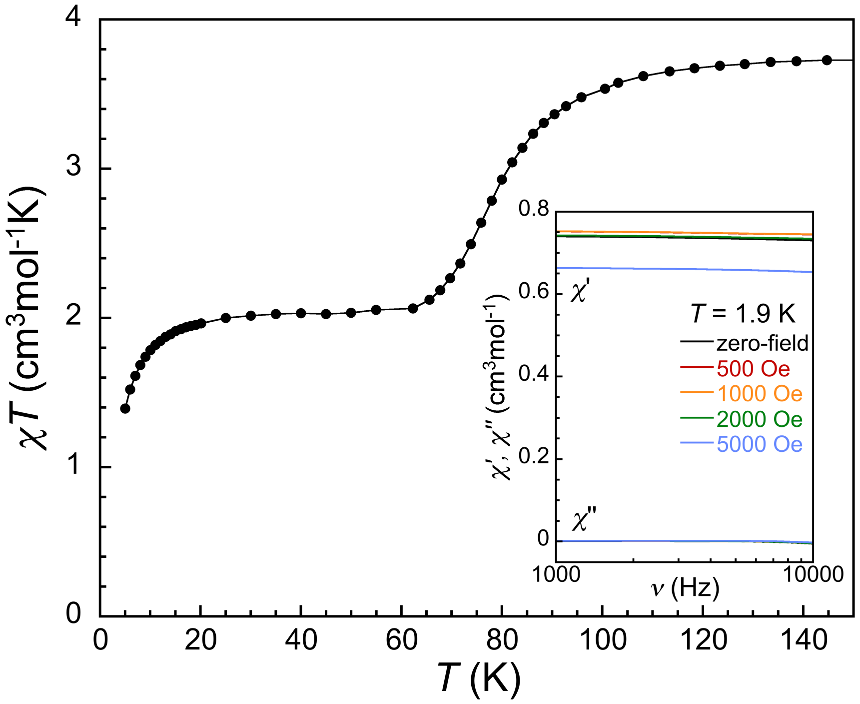

Figure S8. Temperature dependence of the χT product of polycrystalline [Fe(mtz)$_6$](BF$_4$)$_2$ (**3**) as derived from *dc* measurements at 0.3 K/min and 0.5 T applied *dc* field. Inset: Frequency dependence of the in-phase and out-of-phase components of the *ac* magnetic susceptibility of **3** at 1.9 K under the indicated applied *dc* fields, showing no detectable out-of-phase signal at any applied field. The *ac* field amplitude was 4 Oe.

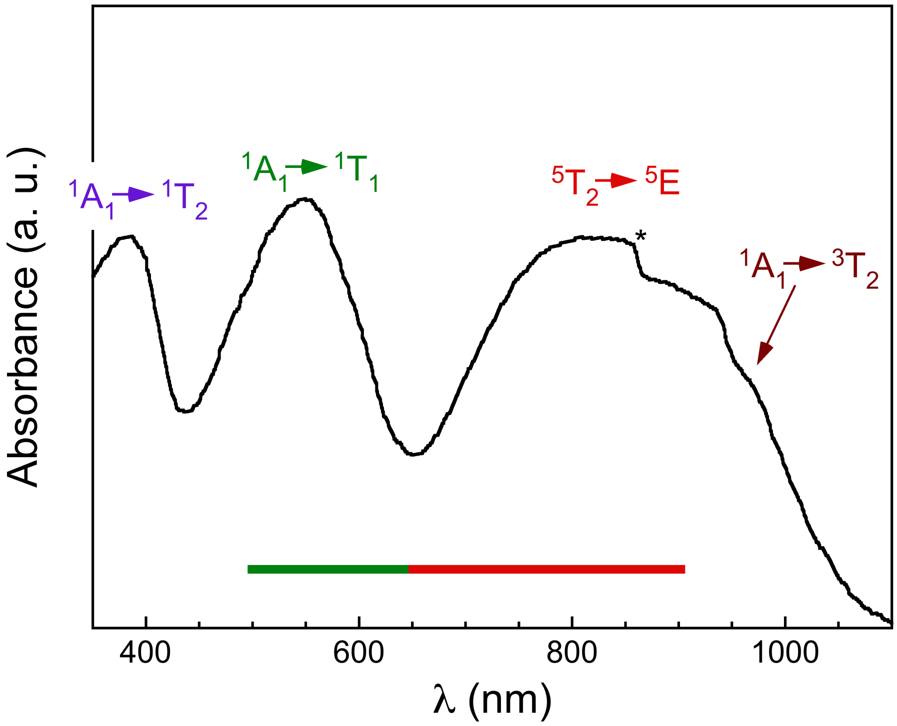

Figure S9. Diffuse reflectance solid-state absorption spectrum at *ca.* 77 K for polycrystalline $[Fe(mtz)_6](CF_3SO_3)_2$ (**2**). The main transitions associated with the LS ($^1A_1 \rightarrow {}^1T_1$ and $^1A_1 \rightarrow {}^1T_2$) and HS ($^1A_1 \rightarrow {}^3T_2$) sites are indicated, including the weak and broad spin-forbidden $^1A_1 \rightarrow {}^3T_2$ LS band as expected from data on single crystal of the analogue compound $[Fe(ptz)_6](BF_4)_2$.[7] The discontinuity indicated by a * is due to a mirror switch. Horizontal red and green thick lines depict the wavelengths ranges used respectively for the red and green broad-band irradiation.

[7] a) A. Hauser, *Chem. Phys. Lett.* **1986**, 124, 543; b) A. Hauser, *J. Chem. Phys.* **1991**, 94, 2741